Speaking in mixed signals: Aperiodic activity in visual processing

A.R. D'Argence[1*], M.W. Preston[2], C. Cazares[1], Bradley Voytek[1-4]

[1]Department of Cognitive Science, [2]Neurosciences Graduate Program, [3]Halıcıoğlu Data Science Institute, [4]Kavli Institute for Brain and Mind, University of California, San Diego, La Jolla, CA, USA 92093.

*e-mail: aruizdargence@ucsd.edu

Data availability
All code used for analyses and plots is publicly available on GitHub at https://github.com/voytekresearch/v1_v4_1024_elec.

Acknowledgements
We thank Chen, Morales-Gregorio and company for sharing both raw and processed data for our analysis.

Author contributions
A.R.D. and M.P. wrote the analysis code and analyzed the data. C.C. and B.V. advised analyses. A.R.D. and M.P. wrote the manuscript, and all authors edited the manuscript.

Competing interests the authors declare no competing interests.

Abstract

The role of transient event-related potentials (ERP) and neural oscillations in cognitive processes such as vision and attention have long been studied; however, recent human intracranial EEG studies have highlighted the presence of dynamic shifts in aperiodic activity in response to visual stimulation. Despite burgeoning interest in the functional role of aperiodic neural activity, the biophysical mechanisms have not been fully characterized. Non-human primate (NHP) models allow us to investigate the cellular underpinnings of LFP activity; however, anatomical differences in visual cortices between human and NHP models might cause differences in stimulus-evoked visual processing. Here, we apply Spectral Parameterization to analyze aperiodic responses to visual stimulation in macaques. We show that the aperiodic exponent and offset of the LFP power spectra both increase upon stimulus presentation and show a slow decay after onset. These changes manifest as a broadband upward shift and steepening of the power spectra. Furthermore, we show that these spectral changes are correlated with local multiunit activity (MUA) across time, supporting previous findings linking broadband spectral power to local spiking activity. These findings suggest that aperiodic activity is functionally relevant for visual encoding and linked to the underlying biophysics, indicating that primates may be a good model for studying the cellular mechanisms of visual processing.

Introduction

Natural scenes in the visual world are composed of complex objects, textures and colors that, through higher order visual processes, give rise to our perceived reality [1–4]. These visual inputs can be quantified through electrophysiological patterns of brain activity which aggregate synchronous, rhythmic oscillations with aperiodic activity as a representation of population firing [5,6]. Local field potential (LFP) recordings permit the individual measurement of oscillatory and aperiodic activity [7]. Importantly, aperiodic activity has been recently linked to the dynamic balance between neural excitation and inhibition as well as temporal precision in sensory integration processes [8,9]. Disruption in this balance has been implicated in neurological disorders such as epilepsy, schizophrenia, and autism [10–13].

Recent human intracranial electroencephalography (iEEG) studies have highlighted the presence of dynamic shifts in aperiodic activity in response to visual stimulation [14]; however, the biophysical mechanisms underlying the functional role of this activity have not been fully characterized. Non-human primate (NHP) models allow us to investigate the cellular underpinnings of these electrophysiological patterns due to shared neurological features not found in other animals [15]. However, anatomical differences in visual cortices between human and NHP models might cause a difference in stimulus-evoked visual processing [16,17]. We parameterized stimulus-evoked changes in aperiodic electrophysiological activity in the macaque visual cortex to establish whether LFPs in the primate visual cortex exhibit event-related changes in aperiodic activity, and characterize the biophysical mechanisms of these aperiodic shifts.

We hypothesize that the presentation of visual stimuli will cause event-related changes in aperiodic activity. Specifically, due to the potential link between aperiodic activity and the dynamic nature of neural firing reflected in LFP activity, we hypothesize that visual stimuli will cause a flattening of the LFP power spectrum, signaling excitatory drive. To investigate this hypothesis, we leveraged an openly available dataset of LFP recordings collected from two macaques implanted with 1024 electrodes across the primary visual cortex (V1) and supplementary visual area V4 as they engaged in a visual fixation task (Chen et al., Scientific Data, 2022). We performed time-resolved spectral decomposition and parameterization of LFP responses, and observed dynamic fluctuations in aperiodic activity in response to visual stimulation. We show that the aperiodic exponent and offset of the LFP power spectra both increase upon stimulus presentation and show a slow decay after onset. These changes manifest as a broadband upward shift and steepening of the power spectra. These effects were widespread across recording electrodes in V1 and V4. Furthermore, we show that these spectral changes are correlated with local multiunit activity (MUA) across time, however, our results indicate a negative correlation in contrast to previous findings linking broadband spectral power to local spiking activity. These findings suggest that aperiodic activity is functionally relevant for visual encoding and linked to the underlying biophysics. Thus supporting the primate visual cortex as a model for studying the cellular mechanisms of stimulus-evoked aperiodic shift, though further investigation is still needed. Decoding the biological mechanisms that give rise to visual processing may provide insight into how the brain processes information in cognition and disease.

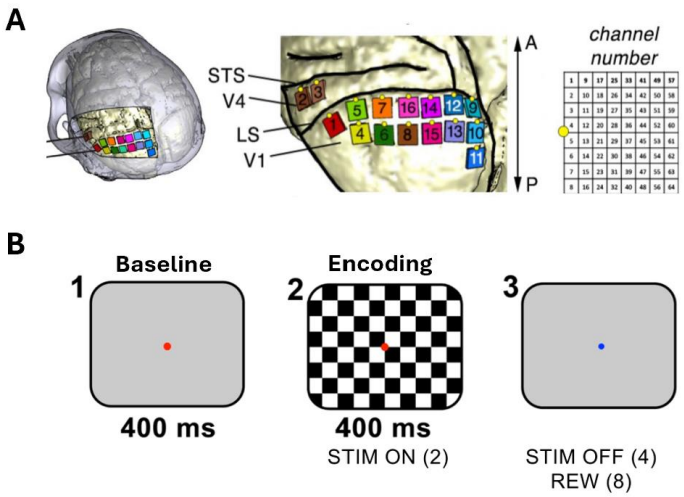

Fig. 1| Experimental paradigm. a, Array placement spanning V1 and V4, including channel position for all arrays. **b**, Visual fixation task performed each trial for both monkeys while head-fixed. The visual stimulus is a static checkerboard pattern filling the entire screen for 400 milliseconds.

Methods

Dataset

Electrophysiological recordings were collected by Chen et al.[18]. The dataset consists of high-resolution, large-spatial V1 and V4 cortical activity in two macaque monkeys. Neuronal activity was recorded with a 1024-channel intracranial implant distributed across 16 Utah electrode arrays, with 64 electrodes each. Two arrays were implanted on V4 and the remaining (n=14) on V1 (Fig. 1a). Data was sampled at a rate of 30 kHz. LFP and MUA recordings were obtained from a behavioral task collected across three recording sessions per animal. The published report contains the complete details on data collection procedures, experimental design, and data preprocessing.

Visual fixation task: Each session consists of at least 30 trials. For each trial, the monkey maintained fixation on a grey screen for 400 ms before a checkerboard stimulus appeared for another 400 ms (Fig. 1b). Following, the experimenters determined signal-to-noise ratio (SNR) by comparing the visually evoked activity on each channel to baseline. This metric was meant to serve as an assessment of the quality of the neuronal signal, however, for our analysis we included all channels independently of their SNR score. Sessions were then epoched into baseline and encoding segments for spectral analysis.

Data preprocessing was done by the experimenters after the recording session. Raw neuronal data was temporally aligned to extract LFP and envelope multiunit activity (MUAe). The LFP signals were generated with a low-pass Butterworth filter at 150 Hz and down-sampled to 500 hz. MUAe is defined by the experimenters as the aggregation of spiking activity across

multiple units recorded via one electrode. To generate the MUAe, the experimenters filtered the raw data between 0.5–9 kHz. The filtered signal was rectified which was then followed by a low-pass Butterworth filter of 200 Hz. The data were down-sampled by a factor of 30 and a final bandstop filter was applied at 50 Hz.The LFP signals were generated with a low-pass Butterworth filter at 150 Hz and down-sampled to 500 hz.

Spectral Analysis

Power spectra were calculated using the MNE toolbox v.1.3.1[19]. Each trial consisted of a baseline (-0.3–0 seconds) and encoding (0–0.3 seconds), from which the spectral analysis was performed. The multitaper method was applied to compute spectral estimates for short-time windows balancing the bias-variance tradeoff. For the epoch based analysis, the function mne.time_frequency.psd_array_multitaper was applied to calculate the spectral content for each electrode in baseline and encoding. For our time-resolved analysis, we implemented the function mne.time_frequency.tfr_array_multitaper. The general settings were used for parameterization: peak width limits: (2, 12); maximum number of peaks: 5; peak threshold: 2.0; aperiodic mode: 'knee.'.

Spectrograms were computed for both baseline and encoding epochs for each trial using multitapers. For the time-resolved analysis, the frequency range selected was 4–100 Hz; a window of 300 ms; and a bandwidth of 10 Hz. Trials were averaged for each electrode and aggregated across arrays.

Parameterization

For each channel, power spectra were parameterized using the open-source toolbox developed by [6], v.1.1.1. This approach models the power spectrum as a combination of oscillatory and aperiodic components, allowing further analysis of aperiodic components alone. The power spectral density $P(f)$ at each frequency f is the sum of the aperiodic component $L(f)$ and oscillatory components $G_n(f)$:

$$P(f) = L(f) + \sum_{n=0}^{N} G_n(f)$$

The aperiodic component by itself can be modeled as a Lorentzian function with offset b, spectral knee k, and aperiodic exponent X:

$$L(f) = b - log[k + f^X],$$

While the oscillatory components are modelled as Gaussian functions. Since we plotted the power spectrum on a log-log axis, the fit will be slightly bent due to the aperiodic mode selected ('knee'), affecting the aperiodic exponent X which otherwise in the 'fixed' mode would solely correspond to the slope of the spectra. This approach assumes that oscillatory and aperiodic processes are distinct and separable.

Statistical analysis

Statistical analyses were carried out using the NumPy and SciPy.stats Python packages. We calculated the mean, variance, and standard deviation for our epoch-based analysis. During the baseline period, we applied a KS test for normality and a paired t-test for the difference before and after stimulus presentation for both the aperiodic offset and exponent.

A linear regression was used to evaluate whether shifts in aggregated spiking activity, denoted by MUAe, were related to shifts in the aperiodic offset and exponent. A scatter plot was overlaid to show individual electrode values across-trial average.

Results

Our analysis examined whether macaques exhibit stimulus-evoked changes in aperiodic activity during visual processing. To quantify these aperiodic features, we analyzed the spectral composition of LFP signals before and after visual stimulus presentation. The aperiodic component of the power spectrum is modeled using a Lorentzian function, characterized by a broadband offset, knee, and aperiodic exponent. Previous studies have linked the aperiodic exponent, which reflects the slope of the power spectrum, to the balance between synaptic excitation and inhibition. While the broadband offset has been associated with population firing rate. Considering these findings, our analysis focused on stimulus-evoked changes in the aperiodic exponent and offset.

Functional

First, we show voltage changes in the time-series of single trials upon stimulus presentation marked at 0 seconds (Fig. 2a). To calculate the power spectrum, we averaged across all trials and fitted the Spectral Parameterization model (Fig. 2b). Here, the peaks at 60 and 120 Hz are line noise, most likely repeating due to harmonics. Offset and exponent values were extracted at baseline for every electrode placement in each of the two subjects (Fig. 2c-f). The schematics show example values for one monkey while the histograms include both subjects. For monkey ‘A’, in the visual task session ‘SNR_140819’, the aperiodic offset displayed a mean of 5.742 and variance of 0.427; the KS test results showed a value of 0.082 and p-value of 0.000. The mean for the aperiodic exponent in the same subject and session was 2.179 with a variance of 0.103; the exponent KS test results were 0.179 with 0.000 in p-value. For the second monkey, ‘L’, session ‘SNR_250717’, the offset displayed a mean of 6.192 and a variance of 0.374; for this variable, there was a value of 0.045 on KS test and 0.032 in p-value. Furthermore, the aperiodic exponent for this monkey and session had a mean of 2.091 and 0.068 variance; the KS test had a value of 0.038 and p-value of 0.105.

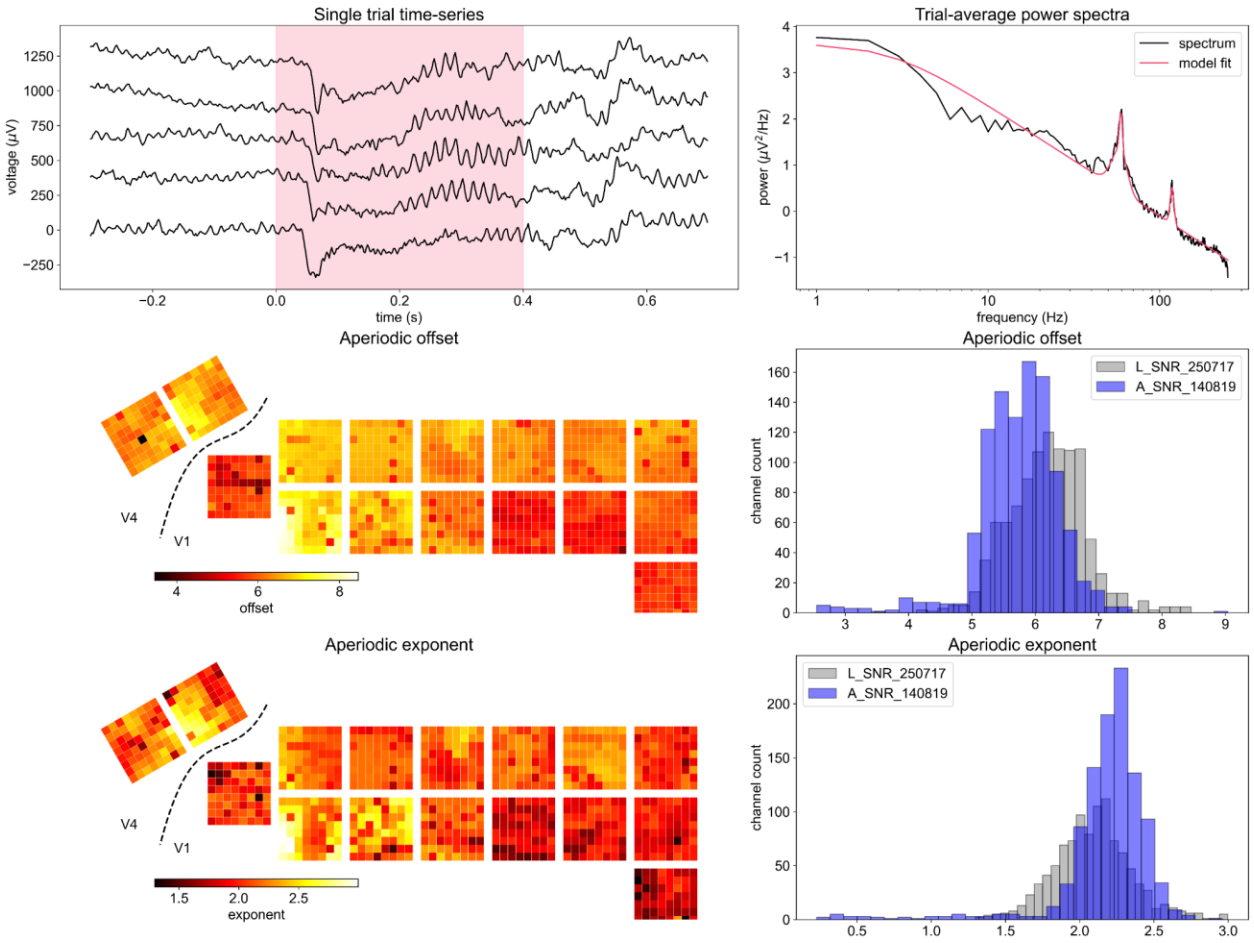

Fig. 2| Baseline aperiodic activity in macaque visual cortex. a, Time-series representation of electrophysiological recordings across single trials for an example channel. **b**, Trial-averaged power spectrum for one subject with aperiodic model fit superimposed. **c, d**, Schematic of array placement displaying baseline aperiodic offset (**c**) and exponent (**d**). **e, f**, Histogram displaying baseline aperiodic offset (**e**) and exponent (**f**) for all channels.

For each aperiodic component, we compared the baseline (-0.3–0 seconds) values with the average across trials during encoding (0–0.3 seconds). We plotted a spectrogram of an example session (Fig. 3a) and computed the epoched change in overall power spectra between baseline and encoding (Fig. 3b). We have shaded the variance in the spectral difference between baseline and encoding, which shows an overall increase in power after the visual stimulus was presented (Fig. 3c). Similar to baseline, we extracted the values for aperiodic offset and exponent post-stimulus presentation and calculated the difference between pre and post stimulus for every electrode placement in each of the two subjects (Fig. 3d-g). The change in offset for monkey ‘A’, in session ‘SNR_140819’ had a mean of 0.801 with a variance of 0.228; for this analysis, we implemented a paired t-test with results of -53.588 and p-value of 0.000. The same subject showed a mean change of exponent of 0.294 and 0.043 variance; the t-test results showed -

45.178 and a p-value of 0.000. The second subject, with the same session used to calculate baseline values, had a mean offset difference of 1.163 with a variance of 0.509; t-test of -52.135 and p-value of 0.000. Finally, the change in exponent for this same subject had a mean of 0.373 with a variance of 0.118; t-test of -34.696 and p-value of 0.000.

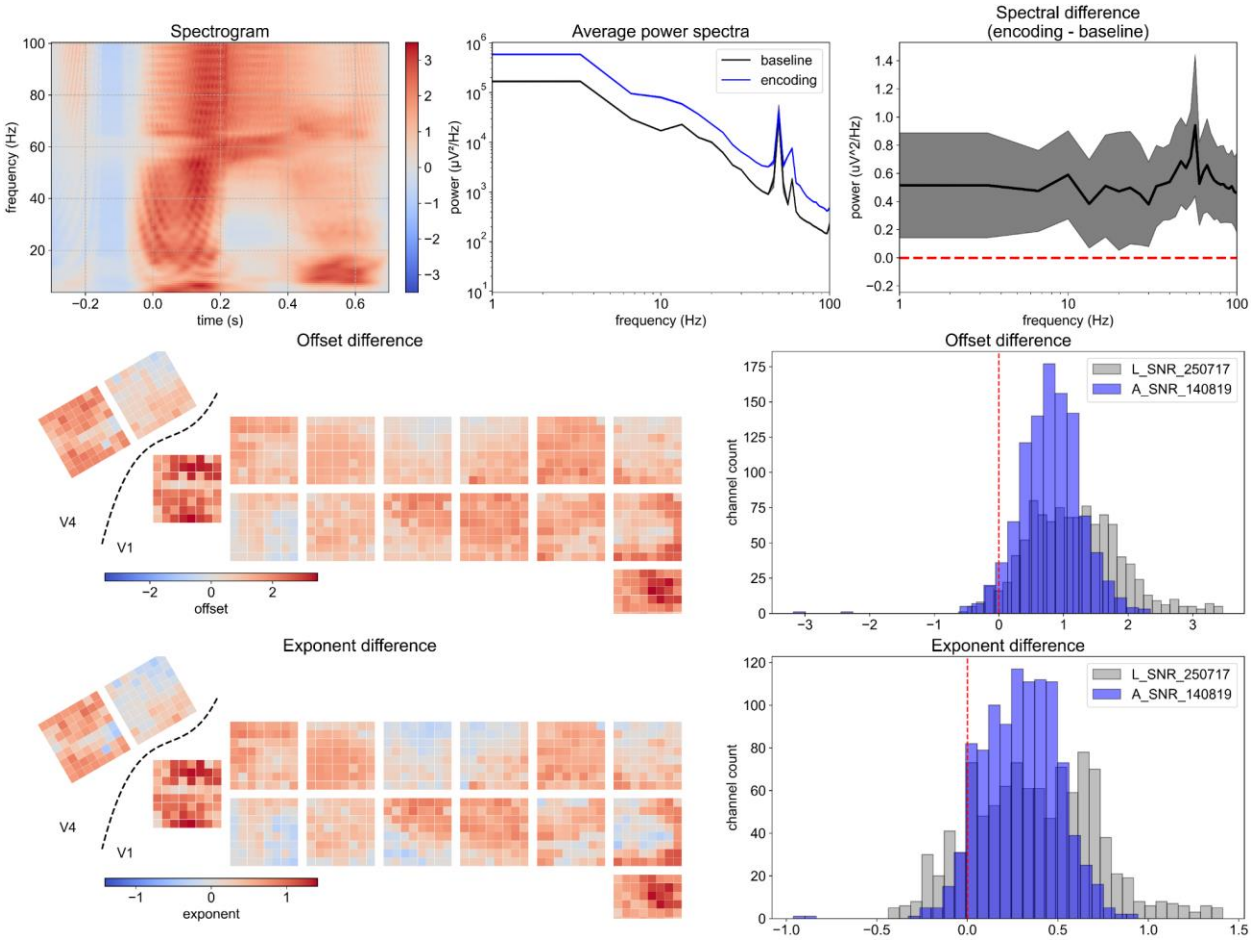

Fig. 3| Aperiodic components display an overall increase upon stimulus presentation. a, Trial-averaged spectrogram displaying change in power across time at all frequencies. **b**, Grand-averaged power spectra for all channels in baseline and encoding epochs. **c,** Difference in power spectra for all frequencies between encoding and baseline epochs. The shaded region represents the standard deviation across channels. **d, e**, Schematic of array placement displaying the difference in aperiodic components between baseline and encoding. **f, g**, Histogram displaying difference in aperiodic components.

Physiological

Biophysical responses, as shown through aggregated spiking activity in MUAe, were computed in epochs to calculate the difference before and after stimulus presentation for each electrode (Fig. 4a). We then proceeded to plot the MUAe in a time-resolved manner alongside the aperiodic offset and exponent (Fig. 4b). Marking time zero as stimulus presentation, the three variables displayed a change in z-score. Finally, we computed a linear regression between the aperiodic components and MUAe, showing that they hold an overall negative correlation. Monkey 'A' displayed a slope of -0.624 when compared to the exponent and -1.112 with offset, holding a p-value of 0.000 for both. For monkey 'L', the slope correlating the exponent and MUA was of -0.259 and for the offset -0.162, with p-values of 0.000 and 0.009 respectively.

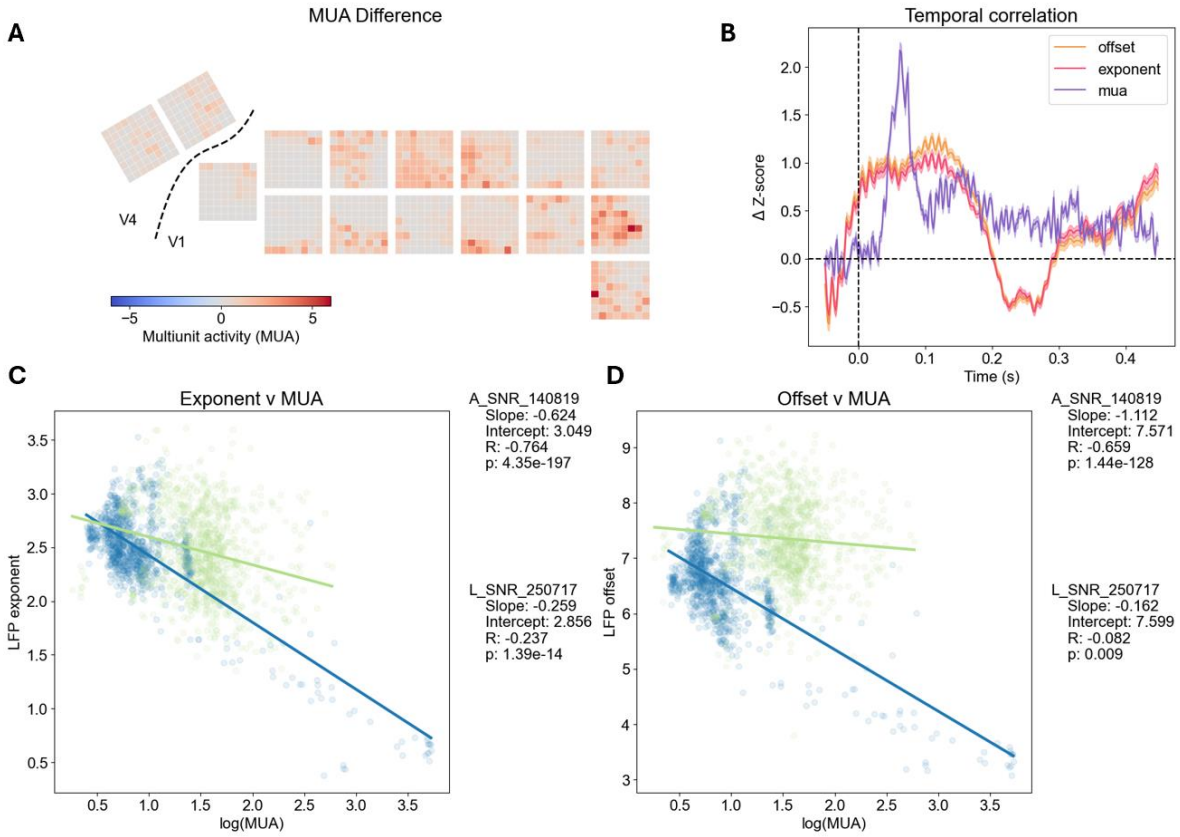

Fig. 4| Time-resolved parameterization of spiking activity with LFP exponent and offset. a, Schematic of multiunit activity across channels displaying the difference between encoding and baseline. **b**, Time-resolved parameterization between all components display changes upon stimulus presentation. **c,** Linear regression shows negative correlation between aperiodic exponent and multiunit activity for both monkeys. **d**, Linear regression shows negative correlation between aperiodic offset and multiunit activity for both monkeys.

Discussion

Physiologically-informed models link aperiodic local field potentials (LFPs) to underlying spiking dynamics. Spectral components such as the aperiodic offset and exponent have been linked to neural firing rate and population balance of excitation and inhibition, respectively [9,20]. Non-human primate (NHP) models may prove useful to gain a better understanding of the biological basis behind these biophysical mechanisms, however, it is unclear if differences in anatomy between humans and NHPs extend to differences in stimulus-evoked visual processing.

In this study, we compared stimulus-evoked changes in LFP and MUA through an epoch-based and time-resolved analysis. Our main aims were to: 1) establish whether LFPs in the primate visual cortex exhibit event-related changes in aperiodic activity, and 2) characterize the biophysical mechanisms of these aperiodic shifts. Our results indicate that macaque LFPs in primary visual cortex (V1) and supplementary visual area V4 exhibit stimulus-evoked changes in aperiodic activity. We show that stimulus encoding is associated with broad increases in the aperiodic offset and exponent, although these shifts seem to vary between subjects. This raises one notable limitation within our study: we are unable to statistically account for inter-subject differences in aperiodic changes due to low subject count (n=2). A possible workaround to this problem would be to inspect each subject's evoked response potentials since variability in subject evoked responses to the stimulus might address the differences we observed in the aperiodic components.

Future studies could address this limitation by looking at the evoked-response potentials (ERPs) from each subject on each session. Since ERPs are voltage changes that directly occur due to a sensorial event, discrepancies between these signals in subjects could explain the difference in aperiodic component changes we saw in our epoch-based analysis. Another route that might be of interest would be to characterize the interaction between aperiodic shifts and oscillations, more particularly alpha band changes after a stimulus presentation given their role in regulating the timing and temporal resolution of visual perception [21]. Finally, one last opportunity for future research would be to analyze if these aperiodic components still display some shift when the subject is in resting state or when switching states such as in arousal. The current dataset contains three resting state sessions for each monkey and pupil diameter data for each session. By investigating and understanding how the brain encodes and interprets visual information, we can gain valuable insights into cognitive function and how they go awry in neurological disorders. This knowledge can inform the design of more precise, personalized healthcare approaches.

References

1. Bertamini, M., Silvanto, J., Norcia, A. M., Makin, A. D. J. & Wagemans, J. The neural basis of visual symmetry and its role in mid- and high-level visual processing. *Ann. N. Y. Acad. Sci.* **1426**, 111–126 (2018).
2. Kinchla, R. A. & Wolfe, J. M. The order of visual processing: “Top-down,” “bottom-up,” or “middle-out”. *Percept. Psychophys.* **25**, 225–231 (1979).
3. Orban, G. A. Higher Order Visual Processing in Macaque Extrastriate Cortex. *Physiol. Rev.* **88**, 59–89 (2008).
4. Sperling, G. Three stages and two systems of visual processing. *Spat. Vis.* **4**, 183–207 (1989).
5. Buzsáki, G. & Draguhn, A. Neuronal Oscillations in Cortical Networks. *Science* **304**, 1926–1929 (2004).
6. Donoghue, T. *et al.* Parameterizing neural power spectra into periodic and aperiodic components. *Nat. Neurosci.* **23**, 1655–1665 (2020).
7. Buzsáki, G., Anastassiou, C. A. & Koch, C. The origin of extracellular fields and currents — EEG, ECoG, LFP and spikes. *Nat. Rev. Neurosci.* **13**, 407–420 (2012).
8. Deodato, M. & Melcher, D. Aperiodic EEG predicts variability of visual temporal processing. *J. Neurosci.* (2024) doi:10.1523/JNEUROSCI.2308-23.2024.
9. Gao, R., Peterson, E. J. & Voytek, B. Inferring synaptic excitation/inhibition balance from field potentials. *NeuroImage* **158**, 70–78 (2017).
10. Dani, V. S. *et al.* Reduced cortical activity due to a shift in the balance between excitation and inhibition in a mouse model of Rett Syndrome. *Proc. Natl. Acad. Sci.* **102**, 12560–12565 (2005).
11. González-Ramírez, L. R., Ahmed, O. J., Cash, S. S., Wayne, C. E. & Kramer, M. A. A Biologically Constrained, Mathematical Model of Cortical Wave Propagation Preceding

Seizure Termination. *PLOS Comput. Biol.* **11**, e1004065 (2015).

12. Symonds, C. EXCITATION AND INHIBITIION IN EPILEPSY. *Brain* **82**, 133–146 (1959).
13. Uhlhaas, P. J. & Singer, W. Abnormal neural oscillations and synchrony in schizophrenia. *Nat. Rev. Neurosci.* **11**, 100–113 (2010).
14. Preston, M., Schaworonkow, N. & Voytek, B. Oscillations and aperiodic activity: Evidence for dynamic changes in both during memory encoding. Preprint at https://doi.org/10.1101/2022.10.04.509632 (2022).
15. Lear, A. *et al.* Understanding them to understand ourselves: The importance of NHP research for translational neuroscience. *Curr. Res. Neurobiol.* **3**, 100049 (2022).
16. Ding, S.-L. Lamination, Borders, and Thalamic Projections of the Primary Visual Cortex in Human, Non-Human Primate, and Rodent Brains. *Brain Sci.* **14**, 372 (2024).
17. Orban, G. A., Van Essen, D. & Vanduffel, W. Comparative mapping of higher visual areas in monkeys and humans. *Trends Cogn. Sci.* **8**, 315–324 (2004).
18. Chen, X. *et al.* 1024-channel electrophysiological recordings in macaque V1 and V4 during resting state. *Sci. Data* **9**, 77 (2022).
19. Gramfort, A. MEG and EEG data analysis with MNE-Python. *Front. Neurosci.* **7**, (2013).
20. Miller, K. J., Sorensen, L. B., Ojemann, J. G. & Den Nijs, M. Power-Law Scaling in the Brain Surface Electric Potential. *PLoS Comput. Biol.* **5**, e1000609 (2009).
21. Clayton, M. S., Yeung, N. & Cohen Kadosh, R. The many characters of visual alpha oscillations. *Eur. J. Neurosci.* **48**, 2498–2508 (2018).